TWT's

HUGGINS LABORATORIES, INC.
999 East Arques Avenue
Sunnyvale, California

HUGGINS LABORATORIES, INC.
999 East Arques Avenue · Sunnyvale, California
REgent 6-9330 TWX SUNV 908 U

TO INSERT PAGES, PUSH DOWN LEVER AT LOWER LEFT, SLIDE THE RING MECHANISM UP, AND SWING RINGS TO THE LEFT.

TO CLOSE BINDING MECHANISM, SWING RINGS TO THE RIGHT AND SLIDE THEM DOWNWARD TO THE LOCKED POSITION.

HUGGINS LABORATORIES, INC.
ENGINEERING NOTES
VOL. II, NO. 1 AUGUST, 1960
Huggins Laboratories, Inc. Sunnyvale, California

Measurement of Relative Phase Shift at Microwave Frequencies*

C. A. FINNILA†, L. A. ROBERTS‡, AND C. SÜSSKIND§

Summary—**A method is described for measuring the relative phase shift of microwave devices, such as traveling-wave tubes, which utilizes the serrodyne technique to transfer the measurements into the audio-frequency range. The method is used to measure the phase shift incidental to the variation of the dc potentials applied to the several electrodes of a 2- to 4-kmc traveling-wave tube. This method is particularly useful in coaxial systems, where accurately calibrated phase shifters (and attenuators without phase shift) are not available.**

Introduction

A PROBLEM often encountered, when making relative phase-shift measurements at microwave frequencies through active devices, is the determination of the phase shift between two signals whose relative amplitudes may vary over some dynamic range. In such cases, the common method of comparing the two signals by a measurement in the shift of the null of a standing-wave pattern created by the two signals traveling in opposite direction through a transmission line cannot be conveniently used, because in such cases the minima may not be very well defined. If the relative amplitudes of the two signals differ by 10 db or more, it becomes extremely difficult even to observe a minimum. The system to be described below avoids this difficulty by shifting the measurement to audio frequencies at which such large dynamic ranges can be readily handled with existing instruments. A similar technique has also been used for the measurement of the phase-shift characteristics of ferrites as a function of the applied magnetic field,[1] and although complex, proves to be quite workable and speedy.

In the present instance, the method was (independently) developed in an effort to measure changes in RF phase shift through traveling-wave tubes with changes in the several tube dc-supply potentials. Measurement of over-all phase shift was not necessary; only relative phase-shift measurements were needed.

Phase characteristics of traveling-wave tubes must be known in the design of many systems: keeping incidental phase modulation within specified limits is often an important requirement. For instance, the phase characteristics of a tube can be used to specify stability and hum level for its power supplies. In some cases traveling-wave tubes may be used for phase or frequency modulation, and phase shift must be accurately known.

For the series of phase measurements reported here, the requirements on the phase-measurement system (see Fig. 1) were rather severe; a wide range of phase shifts had to be measured accurately. Because of the number of measurements needed, they had to be taken quickly to make useful results available in a reasonable time. Since the gain of a traveling-wave tube varies greatly for some changes in its supply potentials, it was essential that the phase-measurement system should not be affected by large changes in signal amplitude.

Phase-Measurement System

The key component in the phase-measurement system is a serrodyne frequency translator.[2] This device yields two stable microwave frequencies, f_0 and f_0+1 kc, as shown in Fig. 1. The latter signal is passed through the tube under test and mixed with f_0; the difference frequency of 1 kc exhibits the same phase shift as the microwave signal f_0+1 kc. In this way, the measurement of phase shift can be carried out at the audio frequency by a simple comparison with a standard 1-kc

* Manuscript received by the PGMTT, July 27, 1959.
† Electronics Res. Lab., University of California, Berkeley, Calif. Formerly at Huggins Labs., Inc., Sunnyvale, Calif.
‡ Watkins-Johnson Co., Palo Alto, Calif. Formerly at Huggins Labs., Inc., Sunnyvale, Calif.
§ Dept. of Elec. Engrg., University of California, Berkeley, Calif.
[1] J. B. Linker, Jr., and H. H. Grimm, "Automatic microwave transmission measuring equipment," *Rev. Sci. Instr.*, vol. 28, pp. 559–563; July, 1957.

[2] R. C. Cumming, "The Serrodyne frequency translator," Proc. IRE, vol. 45, pp. 175–186; February, 1957.

Reprinted from IRE TRANSACTIONS *ON MICROWAVE THEORY AND TECHNIQUES* Volume MTT-8, Number 2, March, 1960

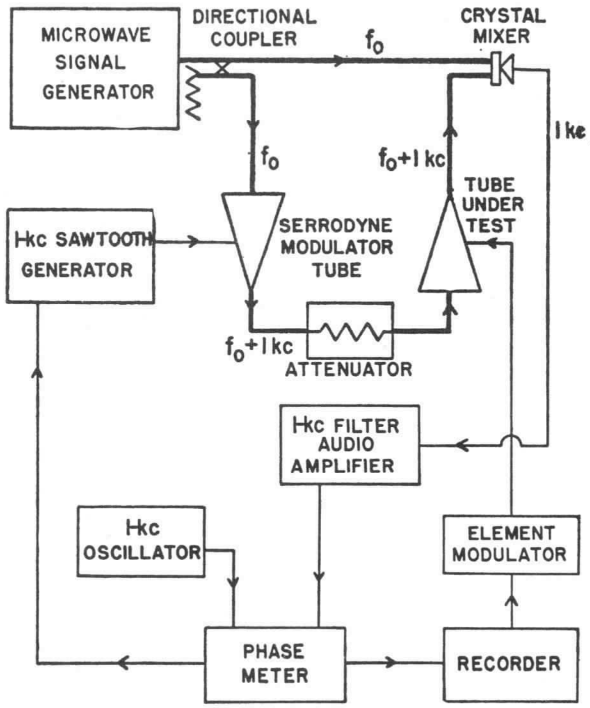

Fig. 1—Phase-measurement system.

oscillator. The principal advantage of the serrodyne technique is that it allows the generation of a phase-stable 1-kc intermediate frequency. A traveling-wave tube of the same frequency capabilities as the one under test can be used for the serrodyne. Serrodyne operation can be best visualized as an approximation to continually increasing phase modulation. If the phase of a signal is increased or decreased at a constant rate, a constant shift in frequency is produced. No known electronic device can continue to increase its amount of phase shift indefinitely, but if phase shift is increased steadily until 2π radians of phase shift has been produced, the instantaneous-signal values will be the same as at 0° phase shift.[3] A quick return to zero at this point produces only a minor disturbance, and phase shift may be continued. Phase shift through many traveling-wave tubes is approximately proportional to helix voltage for phase shifts of well over 2π radians. Moreover, the necessary change in helix voltage does not appreciably change the tube's gain, especially if the tube has more than the customary amount of attenuation between input and output. The serrodyne used here produces a shift of 1 kc in the signal passing through it when its helix is modulated by a 1-kc sawtooth wave of sufficient amplitude to produce 2π radians of phase modulation. All spurious-modulation components are lower by at least 20 db than the shifted signal.

[3] To be sure, a mechanical phase shifter *can* be used to increase phase shift indefinitely, but owing to mechanical limitations can only do so at a rate of a few radians per second, which is not a convenient intermediate frequency.

The path of microwave signals is shown by the thick line in Fig. 1. A conventional signal generator covering the frequency range of the tube under test is used. It is adjusted to give a proper signal input to the crystal mixer to produce linear mixing (1 mw for the crystal used). A directional coupler taps a small part of this signal and sends it through the serrodyne modulator tube. After being shifted in frequency in the serrodyne tube, the signal goes to an attenuator. Enough attenuation is used to insure that the signal at the mixer from this branch of the circuit does not reach a level sufficient to cause nonlinear mixing at any time during a test. For the crystal used, this signal has to be lower by at least 20 db than that from the signal generator. Too much attenuation must also be avoided, since it results in the 1-kc IF signal being too close to noise.

After the attenuator, the signal passes through the tube under test, and then through a directional coupler to the crystal mixer, where a 1-kc sine wave is produced. The 1-kc signal passes through a narrow-band 1-kc filter (to remove spurious harmonic components) and is then amplified and applied to the phase meter. Since the signal often varies in amplitude owing to changes in the gain of the tube during a test, an amplifier with high output capability and low noise level is used. Since the phase meter can operate with signal-input amplitudes changing by ratios as high as 100:1, it is generally not necessary to change gain during a measurement series. The amplifier also has an adjustable phase-shift network which is convenient for setting initial readings.

The phase meter measures difference in phase between the signals at its two inputs. Within the meter, several limiters are used to convert each input signal to a square wave. The metering circuit measures the ratio of the time during which one square wave is positive and the other negative to the total time of the cycle. The meter is calibrated directly in degrees of phase angle between the two inputs. It can be read to within ±0.5° for any amount of total phase shift. With this phase-metering method the input signals can have any waveforms, provided the waveforms are such that they produce square waves with equal positive and negative portions after passage through the limiters. One way to insure that this condition is met is to make the input signals low-distortion sinusoids.

In order to measure relative phase shift, it is necessary to supply a phase reference to the phase meter. This reference is provided by a stabilized 1-kc oscillator. The oscillator has to be quite stable, because any change in its frequency would be converted to a change in phase by the 1-kc filter used in the system. The oscillator output goes directly to the phase meter. As a by-product, the phase meter converts the 1-kc oscillator signal to a square wave. Part of this square wave is used to synchronize the sawtooth generator of the serrodyne frequency-conversion system. By this method, phase-reference information is put into the microwave part of the system.

The remainder of the required system is the unit labeled Element Modulator. This is a special dc power supply that can be placed in series with any of the elements of the tube under test. It is used to vary element voltages to the tube under test by known amounts while relative phase shift is recorded.

Tube Measurement

As an example of the operation of this phase-measurement system, consider the results of measurements made on Huggins Laboratories Type HA-1 traveling-wave tubes. These are 10-mw, magnetically focused, general-purpose traveling-wave tubes capable of operation between 2 and 4 kmc. Five of these tubes were tested to obtain average results.

Relative phase shift as a function of 1) helix voltage, 2) "grid" (actually a gridless beam-forming electrode) voltage, 3) anode voltage, and 4) collector voltage was measured. In addition, changes in phase shift caused by changes in solenoid voltage (causing changes in the magnetic focusing field) were measured. Measurements were made at 2, 3, and 4 kmc. The measurements, which covered a large over-all phase shift, were generally taken twice. The phase-shift control was shifted 90° between the two tests. The average of these two curves tended to cancel out some error from the phase meter as well as errors arising from short-range drift.

Some of the details of the measurement procedure can be illustrated by a brief outline of a typical test. After a sufficient warm-up time, the signal generator is set at the proper frequency and its output to the correct value (1 mw). The proper attenuator is attached. The element modulator is next set for the range of voltages to be used and put in series with the tube element to be tested.

Adjustments of the phase-measurement system are then made, partly with an oscilloscope that is also used to monitor system operation. First, the sawtooth generator is set to 1 kc and synchronized with the 1-kc oscillator. Second, the sawtooth amplitude to the serrodyne tube is set. The oscilloscope is connected to the crystal output before the 1-kc filter. Starting from zero, the amplitude control is slowly increased and the development of the 1-kc sine wave is observed. The amplitude is set for minimum discontinuity in the detected waveform. Next, the 1-kc amplifier gain is set to produce maximum output without distortion when the traveling-wave tube under test is also at maximum gain. (Gain often changes when the voltage to one of the tube elements is changed.) Phase readings are then recorded for different values of voltage on the tube element under consideration.

Experimental Results

The average curves summarize the data best. For the range of grid voltages covered, the change in gain was considerable and signal-to-noise ratios were poor for high values of negative grid voltage. Fig. 2 shows the fair agreement between several tubes as *helix* voltage is varied. Fig. 3 shows the same result, averaged over five tubes, but showing curves at three frequencies.

The data for changes in *collector* and *solenoid* voltages resulted in phase shifts that were small, and showed relatively large variations between tubes, although the general trends were the same.

Phase shifts resulting from changes in *anode* voltage and in *grid* voltage are shown in Figs. 4 and 5, respectively, again for the average of five tubes and at three frequencies. These curves are of considerable practical interest, as variations in either anode or grid voltage are, of course, the common methods of amplitude-modulating the tube. (Phase changes have also been observed as a result of changes in RF drive level, when the dc electrode voltages were fixed. These phase changes were observed not only near the saturation level of the traveling-wave tube, where the effect is well known and is commonly ascribed to nonlinear beam behavior, but also 20 to 30 db below saturation. This observation is an extremely interesting by-product of the present measurement technique.)

Effectiveness and Potentialities of the Measurement System

The relative complexity of the phase-measurement system leads to some problems. The system is very sensitive. One-half degree of phase shift is noticeable. Poor operation of any component of the system leads to noticeable error, especially in the power supplies of both the traveling-wave tube under test and the serrodyne tube. These were electronically regulated power supplies supplied from a regulated ac power source. Despite this precaution, short-term system drift often amounted to 3°. The drift seemed to be related to the power supplies.

The phase meter itself contributed to error. It was rated for ± 2 per cent accuracy, which often amounted to $\pm 3°$. The sign of the error often changed rapidly when crossing 0° or 180° meter readings. This type of error could not be reduced except by extensive alterations of the phase-meter circuits. The error did, however, tend to average out when data were averaged for two phase-measurement tests with 90° of fixed phase shift inserted between them.

Unfortunately, this system could not be checked for accuracy by comparison with a standard, since no

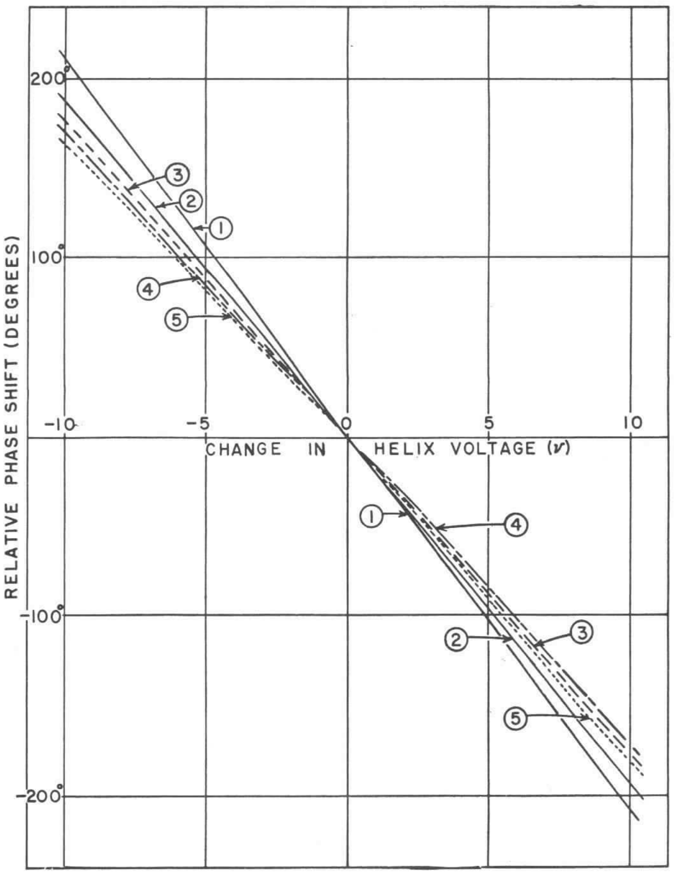

Fig. 2—Phase change for five tubes as a function of helix voltage, at a single frequency (3 kmc).

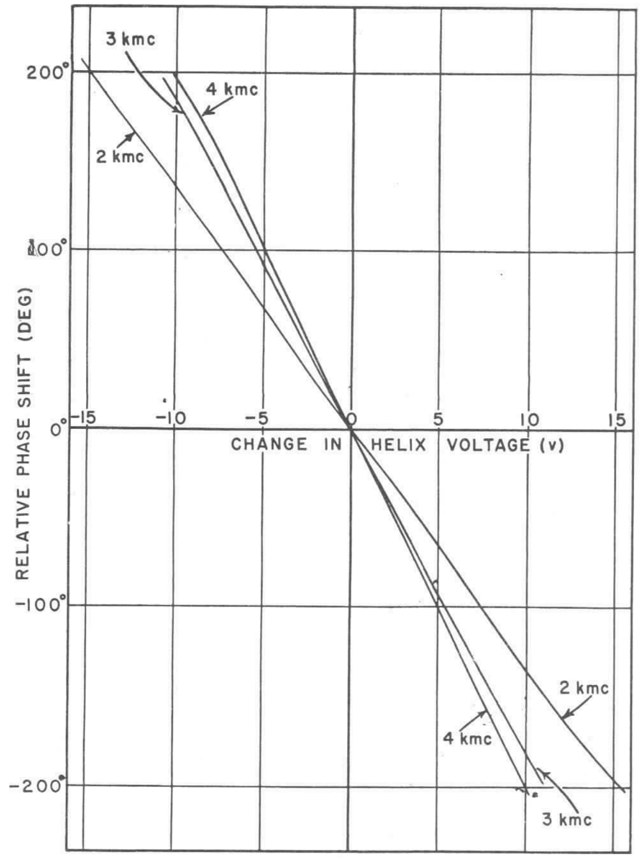

Fig. 3—Phase change for five tubes (average values) as a function of helix voltage, at three frequencies.

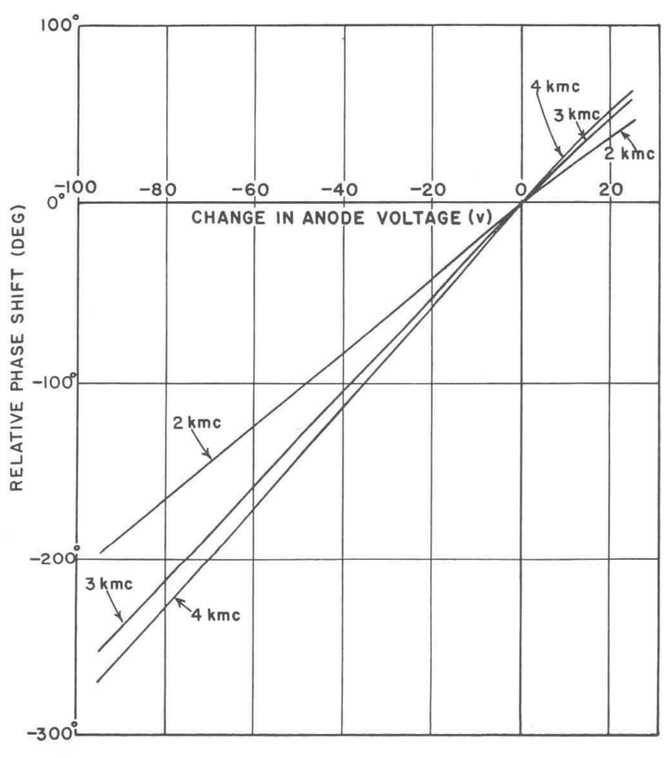

Fig. 4—Phase change for five tubes (average values) as a function of anode voltage, at three frequencies.

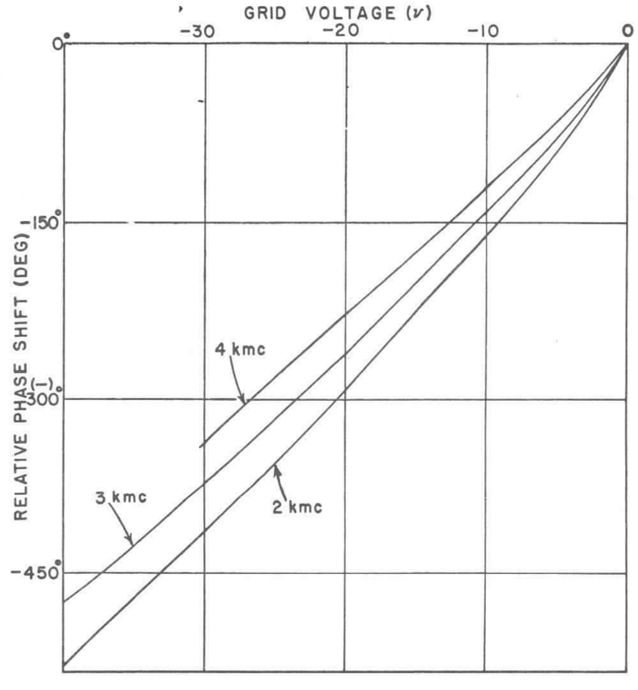

Fig. 5—Phase change for five tubes (average values) as a function of grid voltage, at three frequencies.

standard of sufficient accuracy was readily available. Many of the individual components of the system were checked and corrected. They were thought unlikely to cause noticeable error. On the basis of constancy of results, it is estimated that most of the phase measurements were within $\pm 3°$. While this accuracy is sufficient for many purposes, greater accuracy would be needed for some uses, particularly in attempts to use phase data for a better understanding of the operation of the tube itself. If higher accuracy of phase measurements were necessary, a phase measurement system of this type could probably be constructed to give data accurate to within $\pm 0.5°$. This accuracy would require a different type of audio phase meter and better power supplies.

The primary advantage of this system is its speed of measurement. With manual meter readings, a tube can be completely tested in one day. In addition, the system can be readily adapted to mechanized data collecting. The phase meter could drive a data recorder, with its paper feed driving a potentiometer wired to the element modulator. Thus a phase curve could be recorded directly. The only reason why mechanized data recording was not used in the measurements described above was that the equipment had not yet been completed.

Conclusions

A system of making relative phase measurements at microwave frequencies has been described. It is capable of making these measurements even if the signals to be compared differ widely in amplitude. Although the system is complicated, it can yield data quickly. Many of the components of the system are in rather general use in a microwave laboratory. The audio-frequency phase meter is probably the largest piece of special equipment needed. This system would thus seem to warrant consideration whenever a large number of phase measurements are needed. The system is especially worthy of consideration where traveling-wave or klystron tubes are available for the frequencies of interest.

Examples of phase characteristics of Huggins Laboratories HA-1 traveling-wave tubes have also been given. This tube is typical of many traveling-wave tubes now in use. The curves show that fairly good filtering of traveling-wave-tube power supplies is needed to prevent spurious phase modulation.

Acknowledgment

The aid of R. A. Huggins, who made available the equipment and experimental facilities, is gratefully acknowledged.

Editor's Note

This laboratory is very pleased for the privilege of publishing the foregoing paper. We would be equally pleased to receive similar papers or reports that deal with your experiences and findings on the characteristics and applications of traveling wave tubes.

HUGGINS LABORATORIES, INC.

ENGINEERING NOTES

VOL. II, NO. 2 JANUARY, 1961

Huggins Laboratories, Inc. Sunnyvale, California

LOW-NOISE TRAVELING-WAVE-TUBE AMPLIFIERS

J. C. Stevenson [β]

As the importance of long-range microwave communications increases, the low-noise capability of the traveling-wave tube becomes more significant that ever. Long-range communications usually involves receiving relatively weak signals, and successful reception of such signals requires a high receiver sensitivity.

Receiver sensitivity (commonly measured as tangential sensitivity, i. e., the input signal power that is just equal to the total equivalent input noise of the receiver) depends upon the amount of spurious signals that are generated within the receiver. It then follows that internal noise generation by the receiver must be minimized if weak signals are to be detected. Especially is this true of the first amplifying stage, for receiver noise is largely determined by the noise figure (contribution of noise by the tube) of the input amplifier if the amplifier's gain is such that its noise overrides that of the following stages.

The ability to receive extremely low-level signals is closely allied with the noise bandwidth of the receiver. Many applications hinge upon broadband operation, either for versatility or the capacity to handle large amounts of information. Unfortunately, spurious signal generation increases with bandwidth. To detect weak signals then, we must either decrease the bandwidth or turn to a low-noise broadband amplifying device.

The traveling-wave tube is just such a device. TWT's with maximum noise figures of 5 to 8 db over octave bandwidths have been built, and TWT's having a maximum noise figure of 10 db over an octave bandwidth are readily available. With its low-noise and broadband capabilities, therefore, the traveling-wave tube has no peer as a preamplifier in many applications.

This Engineering Note is concerned with the more general aspects of low-noise traveling-wave tube amplifiers. The difference between thermal noise and tube noise is made, and the more important sources of tube noise are noted. A brief look at the

---

[β] HUGGINS LABORATORIES, INC.

existing noise theory is followed by a short discussion of the factors that influence noise figure. After examining some methods used to reduce TWT noise figures, the individual characteristic of the wave tube is probed.

Thermal And Tube Noise

The noise that exists in any amplifier consists of hum and random noise signals. The former is primarily a power supply problem; random noise signals, however, originate within the tube (tube noise) and its associated circuitry (thermal noise).

Thermal noise

The thermal energy of free electrons in a system's conductors causes a random movement of the electrons that is similar to Brownian motion. Because this movement is random in both time and space, a "thermal noise voltage" is produced.

If tube noise were nonexistent the minimum detectable signal would be set by the thermal noise level. Thermal noise power is expressed as:

$$N_t = KTB \qquad (1)$$

where, K = Boltzmann's constant (watt-second per degree Kelvin)

T = temperature (degrees Kelvin)

B = bandwidth (cps)

When the source and load in a transmission system are matched for maximum power transfer, thermal noise power at room temperature--as computed by equation 1--is 4.0×10^{-21} watts per cycle of bandwidth. A more convenient figure for the thermal noise level at room temperature is -114 dbm per megacycle of bandwidth.

Tube noise

Random motion of the electrons in thermionic vacuum tubes generates noise. Such phenomena as random division of electrons between electrodes and random emission of electrons from the cathode produce this random motion. And noise in a traveling-wave tube depends especially upon the amount of axial velocity fluctuations of the electrons.

Sources Of Tube Noise

Numerous sources of tube noise exist in a traveling-wave tube. Some of the more important are shot, secondary emission, and partition noise. Though it is debatable as to what percentage of total noise generation is accountable to each source, experience shows that none of these sources can be neglected if low noise figures are desired.

Shot noise

A variation in the number of electrons that are emitted by the cathode causes shot noise. The noise is in the form of current fluctuations in the beam that are introduced by the random changes in the time rate of emission of electrons about some mean value.

Secondary emission

Random fluctuations in the number of secondary electrons that are emitted when primary electrons strike one or more of the electrodes generate secondary emission noise. This action increases noise by adding shot current to the beam. Though secondary emission can occur at all positive electrodes, it is most prevalent at the collector.

Partition noise

The radial components of electron thermal velocity give rise to random fluctuations in the division of cathode current among two or more positive electrodes (e. g., helix and collector). These changes in division create partition noise.

Pierce [1] discusses the possibility of another source of noise in a TWT that is analogus to partition noise. Should the aforementioned radial components of thermal velocity alter electron position in the helix, a noise very similar to partition noise may arise--even though no electrons strike the helix.

Nature Of TWT Noise

In 1950 Pierce [1] discussed a simplified noise theory for traveling-wave tubes which predicted that noise in a TWT would take the form of a standing wave along the electron beam. Subsequent experiments by Cutler and Quate [2] produced qualitative agreement with the standing-wave theory.

As a result it is widely accepted that most of the noise generation in a TWT originates at the virtual cathode and that it takes the form of standing space-charge waves. Furthermore, these waves propagate along the electron beam in the same manner as electromagnetic energy propagates along a lossless, nonuniform transmission line.

Three phenomena set up noise standing waves. As the cathode emitts electrons at random, they move away under the influence of an accelerating anode. In so doing, the electrons exhibit minute changes in current density and emission velocity. Current density fluctuations occur in the axial direction only, but variations in emission velocity exist in both the transverse and axial directions. Only axial components contribute to beam noise. It is these current and velocity fluctuations that produce noise standing space-charge waves on the beam.

In addition to current and velocity produced space-charge waves, other waves are set up along the beam by a third phenomenon--perturbations in the beam. Perturbed electrons oscillate at their plasma frequency and give rise to space-charge waves [3]. These waves also apply to the transmission line analogy, an analogy of great importance to the reduction of TWT noise figures.

Factors Affecting Noise Figure

The noise figure (F) for any network or combination of networks is defined by the following equation:

$$F = \frac{(S/N)_i}{(S/N)_o} \qquad (2)$$

where, $(S/N)_i$ = signal-to-noise ratio at the input

$(S/N)_o$ = signal-to-noise ratio at the output

Equations 1 and 2 can be combined with the fundamental gain definition ($G = S_o/S_i$) to express the noise figure in terms of output quantities:

$$F = 1 + (N_a/N_t)_0 \qquad (3)$$

where, N_a = the portion of output noise that is caused by the tube

N_t = the portion of output noise that results from the thermal noise at the input

Many factors contribute to the magnitude of the term N_a in equation 3. Yet to be understood is just how and to what extent all the variables in a TWT influence noise generation, but there are some factors which are fairly well understood. It is to these that we turn our attention.

Input coupler

Because any coupling loss at the input decreases the signal without affecting tube noise, the noise figure in db will be increased by the input coupler loss in db.

Perturbations

As mentioned previously, perturbations in the beam give rise to noise because perturbed electrons, which oscillate at their plasma frequency, set up standing space-charge waves on the electron beam.

Lens action

Electron lenses which are formed by the electrodes in the gun increase both partition noise and velocity fluctuations in a TWT. Already discussed is the fact that both transverse and axial velocity variations are present. In a high-velocity beam, the mean-square transverse velocity fluctuations greatly exceed the mean-square axial fluctuations.

In passing through a lens, the direction of motion of the electrons changes. Because of this action, velocity fluctuations in the axial direction may be changed into transverse fluctuations, and the converse, of course, is also true. As a result it is conceivable that more transverse fluctuations will be converted than axial. Should this be the case there would be an increase in axial fluctuations and noise figure.

Focusing field

The strength of the focusing field has a bearing on lens action and interception. A strong field can reduce lens effect. Partition noise increases in a high-energy beam if the focusing field is too weak. Also, the paths of electron groups from different parts of the cathode will cross should the focusing field be too weak, and if these groups have different velocity distributions, total beam noise increases.

Cathode

Several characteristics of the cathode come under careful scrutiny when we speak of lowering the noise figure. For example, the minimum theoretical noise figure is a direct function of cathode temperature [4]. Electrons that are emitted from a high work function cathode possess high thermal energy, and such emission produces a beam that has a greater velocity spread, more perturbations, and a higher noise temperature. A cathode whose surface is not uniform in density provides patchy or spotty emission which results in nonuniform charge density in the beam. Poor axial emission is caused by a rough emitting surface, and poor axial emission increases velocity fluctuations in the beam. All of these characteristics, either individually or collectively, increase the noise content of the beam

Lowering The Noise Figure

Numerous theories were advanced and many achievements were made by TWT engineers during the last 10 years. Historically, the achievements ran--and still are running--ahead of the theories.

In addition to theories dealing with lens action, perturbations, cathodes, et cetera, several ideas for lowering the noise figure by means of the electron gun were proposed over the years.

Experimental verification of the standing-wave theory by Cutler and Quate prompted the first suggestion: place the gun at some critical distance from the helix, the distance being selected to place a noise standing wave minimum at the entrance to the helix. Such a step did improve noise figures somewhat.

A much greater improvement was realized, however, with Watkins' velocity jump gun [5]. Following came the transmission line analog which led to the exponential gun [6]. The exponential gun represented a major contribution to lowering TWT noise figures, and it was with this gun that much success in the low-noise TWT field was realized. As we shall soon see, recent developments have brought about modifications in the original exponential gun. These modifications have made it possible to make further reductions in TWT noise figures.

The low-noise gun

Present low-noise theory and the transmission line analog make it possible to treat the electron gun as a space-charge wave transformer. The gun functions to match the effective beam impedance at the virtual cathode (potential minimum) to the desired beam impedance at the entrance to the helix. Matching these impedances makes the standing-wave ratio (SWR) of noise current relatively small and places a current minimum at the helix entrance. First order noise theory shows that these conditions give minimum noise figure.

Changing the characteristic beam impedance slowly and smoothly is the best way to match the beam impedance at the potential minimum to that at the helix entrance. An exponential transmission line can perform such an impedance transformation. We choose an exponential transformer because it can match widely different impedances over wide frequency ranges and because it provides a fairly good match over short electrical lengths.

An exponential transformer can be approximated by a properly designed multi-anode or multi-region electron gun. This type of gun is essentially a series of exponential transformers operating in cascade. A typical gun and its potential profile appears in Figure 1.

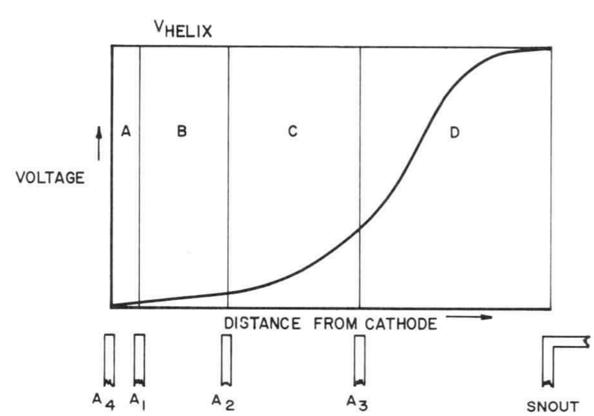

FIGURE 1. POTENTIAL PROFILE AND RELATIVE POSITION OF THE ELECTRODES IN A TYPICAL MULTI-REGION LOW-NOISE ELECTRON GUN.

Low mismatches in all regions of the gun provide a near unity SWR at the helix entrance. In regions B, C, and D, low mismatches are maintained by providing exponential transformations that are not too steep.

The one-dimensional theoretical transformation in region A for a parallel-flow beam is comparatively steep and undesirable. This transformation is based on the assumption that the noise parameters are invariant between the potential minimum and the helix. It has been found, however, that the noise parameters are not invariant in the immediate vicinity of the cathode.

Currie and Forster investigated the effects on beam noiseness of radical changes in the d-c potential distribution in the multi-velocity region near the cathode [7]. Results of their investigation led to a potential profile in region A that differs greatly from the profile previously used in low-noise guns. Figure 2 shows a comparison of the transformation curves prescribed for a one-dimensional beam and Currie's and Forster's "quasi-one-dimensional" beam.

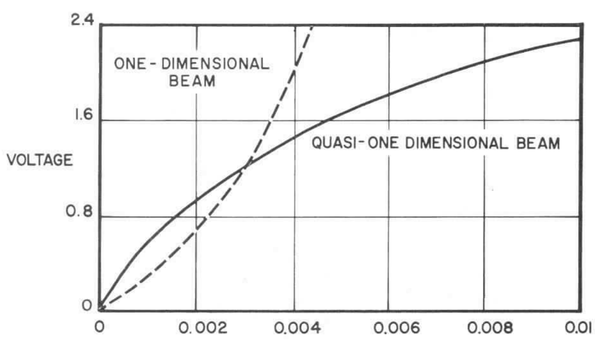

FIGURE 2. COMPARISON OF TRANSFORMATION CURVES IN THE ABSENCE OF SPACE CHARGE, FOR ONE-DIMENSIONAL AND QUASI-ONE-DIMENSIONAL ELECTRON BEAMS.

The Currie-Forster profile exhibits an extended low-velocity region in which the electrons are slowly accelerated immediately after leaving the cathode. In essence, this low-velocity region is considered to be a flexible noise transducer that transforms the variant noise parameters at the potential minimum to the single-velocity region in which the parameters are invariant.

Mueller and Currie calculated the characteristics of noise propagation through a multi-velocity region in which the d-c potential increases linearly [8]. They have shown that beam noiseness decreases as the rate of acceleration decreases in the multi-velocity region. Once the beam leaves the multi-velocity region, however, the single-valued velocity theory of space-charge wave propagation applies, and the previously discussed theory for regions B, C, and D in a multi-anode gun becomes valid.

Several important advantages are inherent in the multi-anode gun: 1) lens effect is reduced since the gun operates without sharp potential discontinuities, 2) the gun lends itself to quantity production because of its mechanical simplicity, and 3) the gun is flexible (i. e., the noise current minimum can be positioned electrically).

In addition to electron gun design, other steps must be taken to combat tube noise.

For example, the input coupler must be designed for minimum coupling loss so that the noise figure will not be greatly degraded. Regardless of the type of coupler used, its parameters are manipulated to give the best possible VSWR (i. e., the best signal transfer to the helix).

As another example, attention is given to the mechanical configuration and chemical composition of the collector with a view toward reducing secondary emission or its effects. The final design often requires that the collector be operated positive with respect to the helix for optimum noise figure.

Other steps taken to lower the noise figure are concerned with focusing and the cathode. Using a strong focusing field reduces lens effect, interception, and perturbations in the beam. Axial and even electron emission is approached by using cathodes with smooth, even-density coatings; high cathode temperatures and high thermal energies are avoided by employing low-work-function emitters such as oxide coated cathodes.

Each TWT Is Unique

In the present state of the art, each traveling-wave tube is an individual. Unlike 6SN7's, 5U4's, and other tubes of that breed, the TWT isn't compatible with direct interchangeability or replacement, for each TWT gives optimum performance under unique operating conditions.

This uniqueness stems from two facts: the electron gun is paramount to low TWT noise figures, and the potential profile associated with the gun is a function of the voltages applied to the anodes. Due to the many variables which influence noise, the anode voltages required to obtain the proper profile usually differ from gun to gun. Improper electrode voltages can, therefore, produce disappointing performance and possibly tube damage.

Accordingly, the manufacturer supplies with each tube a "data sheet" that gives all operating voltages and currents for that tube. Figure 3 shows an example of a data sheet for a Huggins HA-72 which has specified performance of 25 db minimum small-signal gain and 8 db maximum noise figure across the 0.5 to 1.0 kmc frequency range.

The voltages and currents on this data sheet are unique to the particular tube with which the sheet is supplied. The TWT's individuality is stressed by the improbability that another HA-72 will give optimum performance with identical voltages applied. Departure from gun voltages changes the all-important potential distribution of the electron gun and consequently moves the noise-current minimum relative to the helix entrance. Because the specified voltages represent optimum operating conditions, unsatisfactory performance usually results when operating the heater, helix, and collector at other than specified voltages. The dependence of noise figure on operating voltages is discussed in more detail in Note 3, Volume II, of <u>Huggins Engineering Handbook</u>.

There is, of course, a tolerance on the voltage specifications, but system requirements primarily determine the amount of tolerance. All TWT manufacturers are equipped and ready to assist the engineer in attaining best TWT performance in his particular application.

Future Low-Noise TWT Developments

Research in low-noise wave tubes is intense and widespread throughout the industry. Such research is pushing noise figures lower and lower, and in the not-too-distant future we

DATA SHEET

RETURN SHIPMENT OF THIS TUBE NOT ACCEPTED
WITHOUT HUGGINS LABORATORIES APPROVAL.

Tube Type HA-72
Serial No. 000

POWER SUPPLY CONNECTIONS:

WINCHESTER CONNECTOR M9P

- A — ANODE NO. 2
- B — ANODE NO. 3
- C — CAPSULE GROUND
- D — HELIX
- E — HEATER
- F — HEATER
- H — ANODE NO. 1
- J — ANODE NO. 4
- K — CATHODE

WINCHESTER CONNECTOR SMIP IS COLLECTOR CONNECTION.

FREQ.	SMALL SIGNAL GAIN	POWER OUTPUT	GAIN	NOISE FIGURE	
		MEASURED AT: ( )MAX. OUTPUT (x)1 MW INPUT			
KMC	DB	DBM	DB	DB	
0.5	31	5	30	8.0	
0.6	35	5	32	7.5	
0.7	38	6	31	7.8	
0.8	38	6	30	8.0	
0.9	38	6	31	7.8	
1.0	36	4	30	8.0	

OPERATING CONDITIONS:

* $V_{ANODE\ NO.\ 1}$	0
* $V_{ANODE\ NO.\ 2}$	7.3
* $V_{ANODE\ NO.\ 3}$	0
* $V_{ANODE\ NO.\ 4}$	7.2
* V_{HELIX}	81
* $V_{COLL.}$	V_{Helix} + 300
V_{HTR}	6.5

$I_{ANODE\ NO.\ 1}$	--
$I_{ANODE\ NO.\ 2}$	--
$I_{ANODE\ NO.\ 3}$	--
$I_{ANODE\ NO.\ 4}$	--
I_{HELIX}	0
$I_{COLL.}$	0.62 ma
$I_{CATH.}$	0.62 ma
$I_{HTR.}$	0.7 amp

SOL TYPE	BS-26C
$V_{SOL.}$	105
I_{SOL}	4.8 amp
GAUSS	820

*MEASURED WITH RESPECT TO CATHODE.

TESTED BY ____________

DATE ____________

HUGGINS manufacture development engineering design research LABORATORIES

HUGGINS LABORATORIES
999 East Arques Avenue · Sunnyvale, California

F-107

FIGURE 3. SAMPLE "DATA SHEET" FOR A HUGGINS LOW-NOISE TWT AMPLIFIER. SPECIFIED VOLTAGES REPRESENT OPTIMUM OPERATING CONDITIONS.

should see TWT's operating over octave bandwidths with significantly lower noise figures than presently obtained.

Much effort is being devoted to reducing the weight of low-noise TWT amplifiers. Special lightweight solenoids notwithstanding, substantial weight reduction is possible only by eliminating the solenoid.

One method of eliminating the solenoid is to use a straight-field permanent magnet for focusing; solenoid-focused low-noise TWT performance can be duplicated in such a focusing structure. Though PM focusing does lower system weight since no solenoid power supply is required, it may increase tube weight considerably [9]. Therefore, the industry is concentrating on periodic focusing, both magnetic and electrostatic.

Periodic focusing works very well for low and medium power amplifiers. In the present state of the art, however, PPM focusing of "low-noise" TWT's gives, at best, a 12 to 13 db noise figure over a 2 : 1 frequency range. An octave bandwidth noise figure of 25 db represents current achievements with electrostatic focusing. It appears that conflicting field strength requirements for gain and noise figure must be overcome before periodically focused wave tubes will operate over an octave bandwidth with a maximum noise figure of 10 db or less.

Backward wave amplifiers (BWA) form another important phase of low-noise research. Possibilities of extremely low noise figures in the BWA are great, for this type of TWT operates over a comparatively small bandwidth. Yet a BWA still has broadband capabilities since it is voltage tunable over a wide frequency range. Currie and Forster report reproducible maximum noise figures of 6 db for a 25 % tuning range and 4.5 db for a 10 % tuning range [10]. The two apparent problems that must be solved are reducing focusing requirements and limiting gain fluctuations as the tube is tuned.

The history of low-noise traveling-wave tube amplifiers is filled with many, many theories and proposed solutions to reducing noise figures. From each theory and from each solution have come other theories and solutions to push the noise figure progressively lower. This trend is certain to continue until the yet-to-be-determined limiting noise figure in the TWT is reached.

Acknowledgements

The author extends his thanks to D. E. MacKerrow, J. C. Mc Caig, and V. D. Varenhorst for their informative discussions on low-noise traveling-wave tubes.

REFERENCES

1. J. R. Pierce, Traveling-Wave Tubes, D. Van Nostrand Company, Inc., Princeton, New Jersey, 1950.

2. C. C. Cutler and C. F. Quate, "Experimental Verification of Space-Charge and Transit-Time Reduction of Noise In Electron Beams," Physics Review, December, 1950.

3. E. W. Kinaman and M. Magid, "Very Low-Noise Traveling-Wave Amplifier," Proceedings Of The IRE, May, 1958.

4. D. A. Watkins, "Noise At The Potential Minimum In The High Frequency Diode," Journal Of Applied Physics, May, 1955.

5. D. A. Watkins, "Traveling-wave Tube Noise Figure," Proceedings Of The IRE, January, 1952.

6. S. Bloom and R. W. Peter, "Transmission-Line Analog of a Modulated Electron Beam," RCA Review, March, 1954.

7. M. R. Currie and D. C. Forster, "New Mechanism of Noise Reduction in Electron Beams," Journal Of Applied Physics, January, 1959.

8. W. M. Mueller and M. R. Currie, "Noise Propagation on Uniformly Accelerated Multivelocity Electron Beams," Journal Of Applied Physics, December, 1959.

9. "Periodic Permanent Magnet Focused Traveling-Wave-Tube Amplifiers," Huggins Engineering Handbook, Vol. I.

10. M. R. Currie and D. C. Forster, "Low Noise Tunable Preamplifier for Microwave Receivers," Proceedings Of The IRE, March, 1958.

HUGGINS LABORATORIES, INC.

ENGINEERING NOTES

VOL. II, NO. 3 FEBRUARY, 1961

Huggins Laboratories, Inc. Sunnyvale, California

THE EFFECT OF OPERATING VOLTAGE VARIATIONS ON TWT NOISE FIGURE

J. C. Stevenson [β]

As discussed in Note 2, Volume II, "Low-Noise Traveling-Wave-Tube Amplifiers," the traveling-wave tube is an individual, and this characteristic of the TWT cannot be neglected if optimum tube performance is to be obtained. In harmony with this trait of individuality, Note 2 also points out that the manufacturer's prescribed voltages--which represent optimum performance--should be followed. Operation with different voltages usually gives other than optimum performance.

This Engineering Note is concerned with TWT noise figure specifications, the area of investigation being confined to the effect on noise figure of changes in the operating parameters (viz., the focusing field and the collector, helix, anode, and heater voltages). The dependence of noise figure on operating parameters is theoretically analyzed to lay a foundation for understanding the series of noise figure curves which are presented as a part of this Note. These curves graphically illustrate the importance of operating a wave tube with its optimum voltages applied.

An unsophisticated look at three concepts of the low-noise TWT amplifier will lead to an insight of how and why operating parameter changes affect noise figure.

Noise Standing Waves

That most of the noise generation in a wave tube originates at the virtual cathode (potential minimum) and that it takes the form of standing space-charge waves along the electron beam is widely accepted by low-noise TWT engineers. In addition, there is nearly universal agreement that a minimum noise figure for any given tube is theoretically attained when the noise standing wave goes through a minimum at the helix entrance. A standing wave and the critical placement of a standing-wave minimum immediately suggests an impedance matching problem.

[β] HUGGINS LABORATORIES, INC.

The Low-Noise Gun

In its simplest form, a low-noise electron gun can be thought of as a transformer which functions to match the characteristic beam impedance at the virtual cathode to the desired beam impedance at the helix entrance. Such an impedance transformation makes the SWR relatively small and places a standing-wave minimum at the entrance to the helix. More specifically, the electron gun can be treated as an exponential transformer which varies the beam impedance in the following manner:

$$Z = Z_0 e^{k\alpha} \qquad [1]$$

where, Z = characteristic beam impedance

Z_0 = characteristic beam impedance at the virtual cathode

k = "steepness factor"

$\alpha = \beta - \beta_0$ = total phase angle

The total phase angle will prove to be an important factor toward understanding why changes in operating parameters affect noise figure, and it may be defined as:

$$\alpha = \int_{Z_0}^{Z} \frac{2\pi}{\lambda_p}\, dz \qquad [2]$$

where, Z = distance along the beam (Z increases from cathode to collector)

λ_p = plasma wavelength

Because the total phase angle is important, the plasma wavelength or frequency is also essential to the purpose of this Note. The plasma frequency is associated with bunching in the electron beam. As electrons are displaced in the beam to form a bunch, there is a concentration of space charge in the bunch, and this concentration of space charge possesses a corresponding electric field. The electric field produces a restoring force on the electrons that is proportional to their displacement. As a result there is simple harmonic motion of the charge (i.e., the charge oscillates at the plasma frequency).

Without going into the subtleties of plasma frequency and effective plasma frequency, only the infinitely broad electron beam case will be considered. In such a beam the plasma frequency may be defined as:

$$f_p = \frac{1.83 \times 10^8 \, J_0^{1/2}}{2\pi V_0^{1/4}} \qquad [3]$$

where, J_0 = d-c current density

V_o = d-c beam voltage

Noise Temperature

The third and last concept to be examined is that of the noise temperature in the beam, and this will be merely defined as:

$$NT = \frac{f}{f_c} T_k \qquad [4]$$

where, f = frequency of interest

f_c = cyclotron frequency

T_k = cathode temperature

As revealed in elementary physics, the cyclotron frequency is related to the motion of a moving charged particle in a uniform magnetic field. For an electron, the cyclotron frequency may be expressed by the following equation:

$$f_c = \frac{q_e B}{m_e 2\pi} \qquad [5]$$

where, q_e = charge on the electron

m_e = mass of the electron

B = magnetic flux density

Interpreting The Equations

Certain conditions must be set before any correlation between the equations and operating parameter changes can be made. The following discussion will, therefore, be based upon the assumption that the TWT operating parameters are adjusted for optimum performance. Effects on output power and gain are ignored in this discussion since the noise figure is the characteristic of importance.

The impedance transformation between virtual cathode and helix entrance, according to equation 1, is dependent on the total phase angle, α, among other factors. From a matched condition, any change in α will 1) cause an impedance mismatch, 2) increase the SWR of the noise standing wave, and 3) move the standing-wave minimum relative to the helix entrance. These actions, of course, produce a change in the noise figure.

Equation 2 shows that α is a function of λ_p which, as stated in equation 3, is dependent upon current density and beam voltage. Changing the helix, heater, or any anode voltage will naturally affect the current density, the beam voltage, or both. It them follows that the noise figure is a function of a TWT's operating potentials. Though neither the current density or beam voltage is affected by a change in collector potential, the collector voltage does influence secondary emission. Thus, we would expect the noise figure to vary somewhat with a change in the collector voltage.

A glance at equations 4 and 5 instantly reveals that the noise figure varies with heater voltage and, in addition, the focusing field. The former determines cathode temperature and the latter determines the cyclotron frequency.

These equations in no way indicate the relative effect on noise figure of the various parameters, but the following noise figure curves do show that some parameters have more effect on noise figure than do others.

Noise Figure Curves

Noise figure data is presented on four Huggins low-noise amplifiers: a L-band HA-14, a S-band HA-37, a C-band HA-47, and a Ku-band HA-43. All four tubes provide 25 db minimum small-signal gain and 1 mw minimum power output over their specified frequency ranges. The HA-14 and HA-47 have maximum noise figures of 10 db over the 1.0 to 2.0 kmc and 4.0 to 8.0 kmc bands respectively. A maximum noise figure of 11 db across the 2.0 to 4.0 kmc range is attained with the HA-37, and the HA-43 has a maximum noise figure of 17 db over the 12.0 to 18.0 kmc band.

Each series of noise figure data was taken with the tube optimized for broadband gain, power output, and noise figure. The curves shown in Figures 1, 2, 3, and 4 are not presented as being typical of the applicable tube type, but they are representative of the fact that noise figure normally varies with each operating parameter.

In a few cases a curve appears to be inconsistent with low-noise theory. For example, the noise figure should decrease to a limiting value as the focusing field increases. But the HA-37 and HA-43 data shows an increase in noise figure as the field is increased beyond its optimum value. Though contrary to theory, this phenomenon has no adverse effect on tube performance. At any rate inconsistencies do exist and provide further support to the fact that each TWT is indeed an individual.

Acknowledgments

The author expresses his appreciation to J. C. McCaig and V. D. Varenhorst for their helpful suggestions and for their illuminating discussions on the relationships between TWT noise figure and operating parameters.

THE EFFECT OF OPERATING VOLTAGE VARIATIONS ON TWT NOISE FIGURE

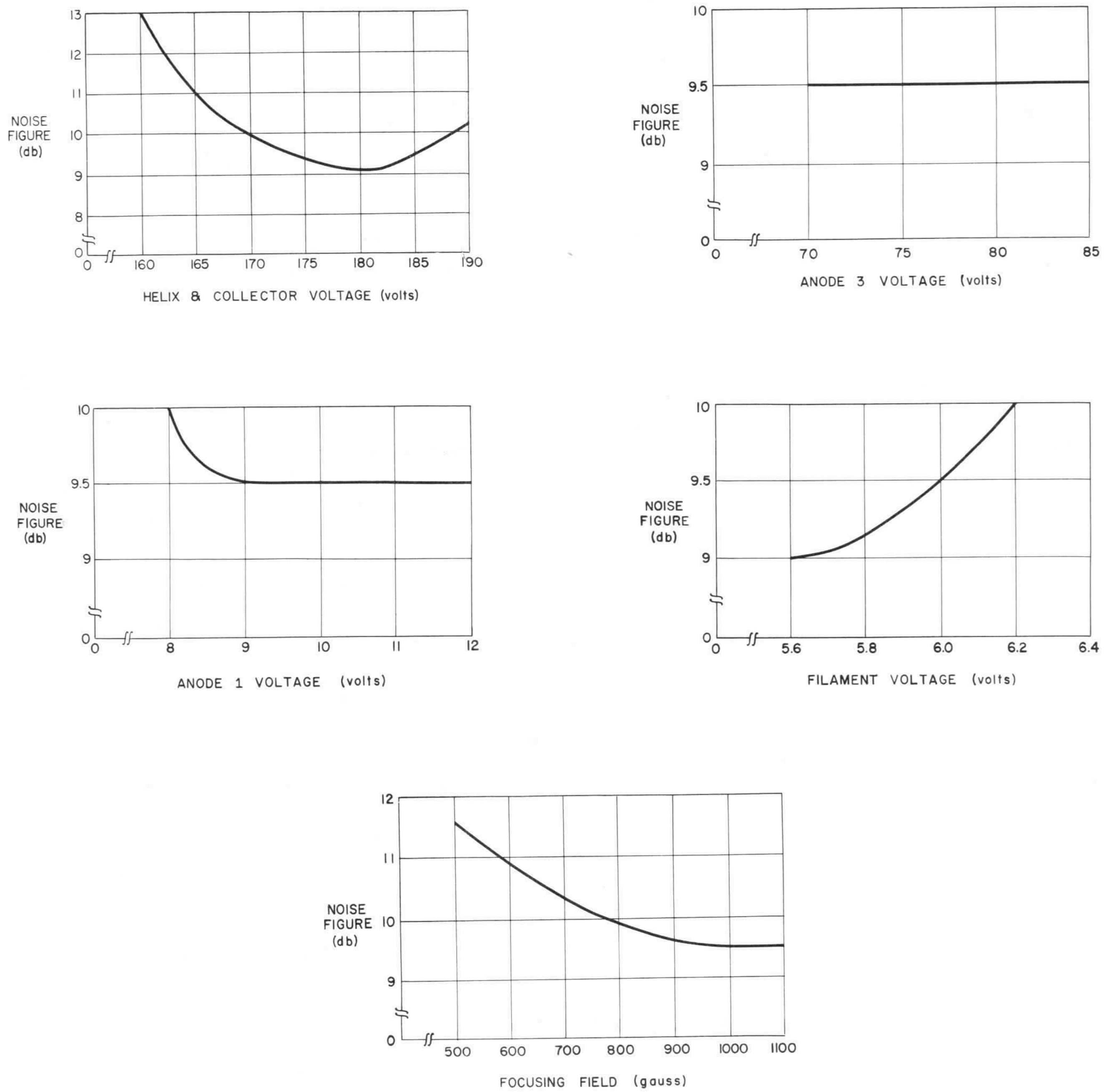

HA – 14 (DATA TAKEN AT 1.5 KMC)
FREQUENCY RANGE, 1.0 TO 2.0 KMC; NF, 10 DB MAX; S–S GAIN, 25 DB MIN; POWER OUTPUT, 0 DBM MIN

OPTIMUM PARAMETERS

V_{A1} = 10 V, V_{A2} = 0 V, V_{A3} = 80 V, V_{A4} = 0 V, V_H = 186 V, V_C = 186 V, V_F = 6.0 V, AND B = 1100 GAUSS

FIGURE 1. HA – 14, NOISE FIGURE VS. OPERATING PARAMETERS

THE EFFECT OF OPERATING VOLTAGE VARIATIONS ON TWT NOISE FIGURE

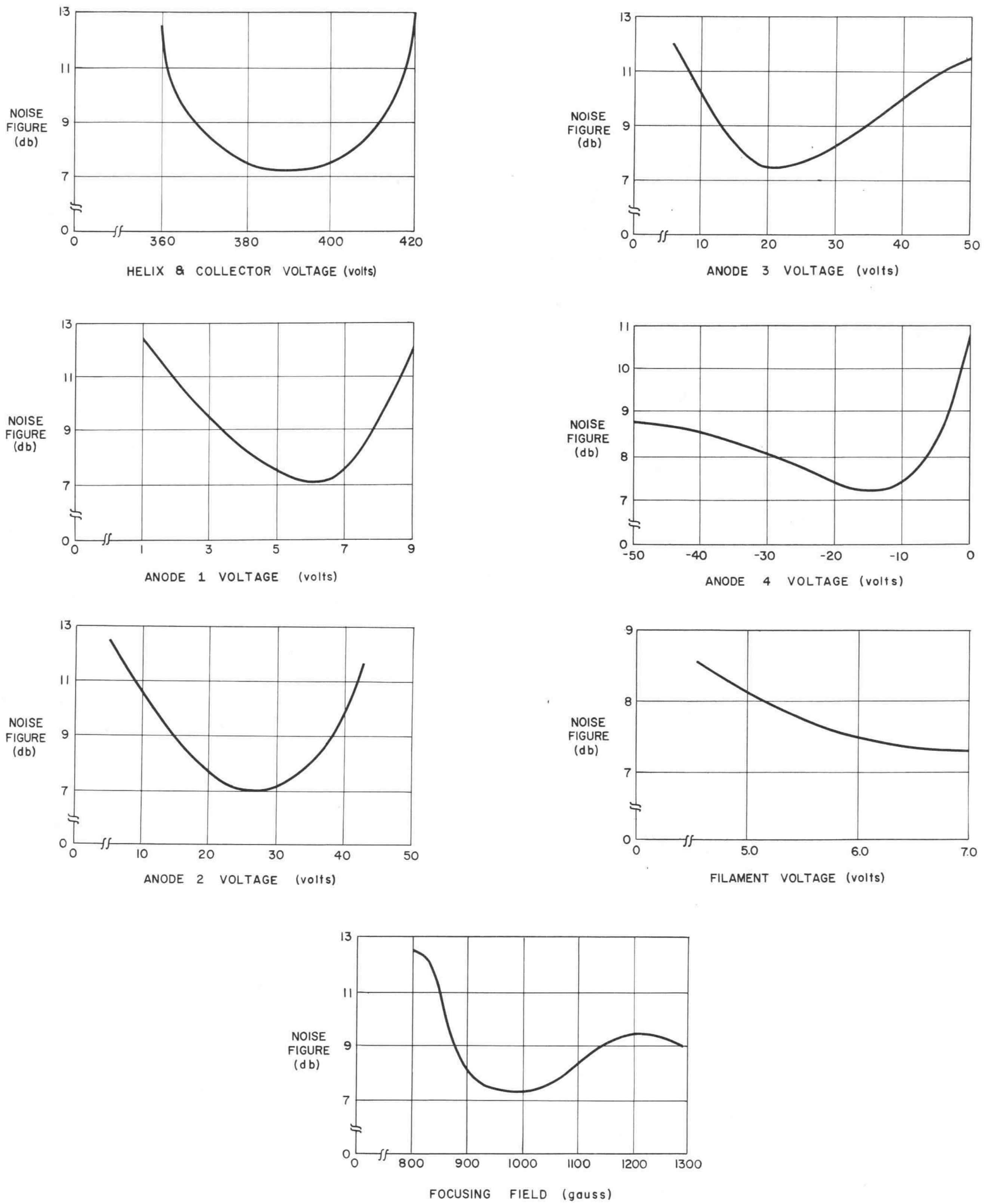

HA – 37 (DATA TAKEN AT 3.0 KMC)

FREQUENCY RANGE, 2.0 TO 4.0 KMC; NF, 11 DB MAX; S-S GAIN, 25 DB MIN; POWER OUTPUT, 0 DBM MIN

OPTIMUM PARAMETERS

$V_{A_1} = 5$ V, $V_{A_2} = 21$ V, $V_{A_3} = 21$ V, $V_{A_4} = -20$ V, $V_H = 400$ V, $V_C = 400$ V, $V_F = 6.3$ V, AND B = 1000 GAUSS

FIGURE 2. HA – 37, NOISE FIGURE VS. OPERATING PARAMETERS

THE EFFECT OF OPERATING VOLTAGE VARIATIONS ON TWT NOISE FIGURE

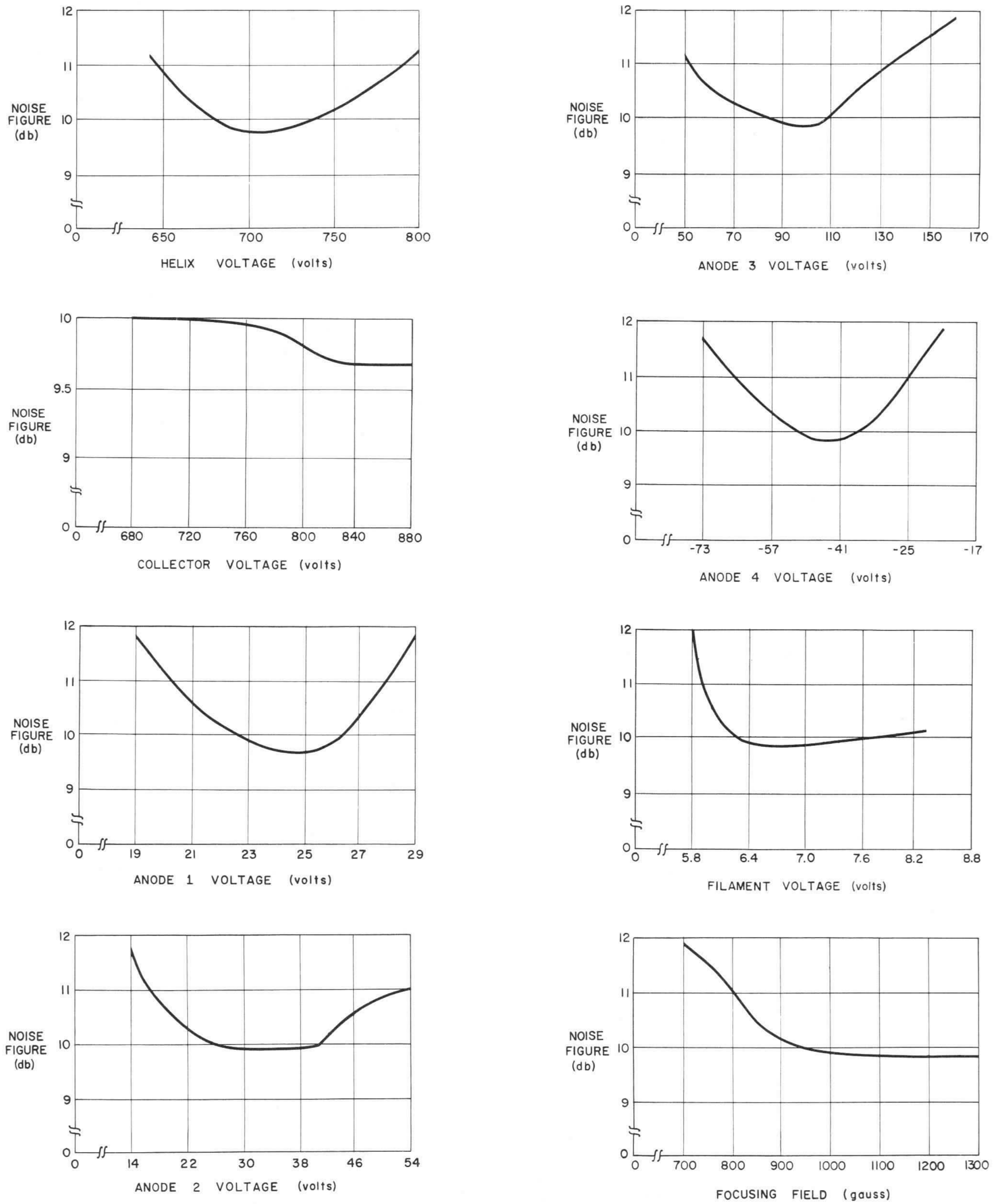

HA – 47 (DATA TAKEN AT 4.0 KMC)
FREQUENCY RANGE, 4.0 TO 8.0 KMC; NF, 10 DB MAX; S–S GAIN, 25 DB MIN; POWER OUTPUT, 0 DBM MIN

OPTIMUM PARAMETERS
V_{A_1} = 23 V, V_{A2} = 36 V, V_{A3} = 102 V, V_{A_4} = –49 V, V_H = 680 V, V_C = 780 V, V_F = 6.3 V, AND B = 1000 GAUSS

FIGURE 3. HA – 47, NOISE FIGURE VS. OPERATING PARAMETERS

THE EFFECT OF OPERATING VOLTAGE VARIATIONS ON TWT NOISE FIGURE

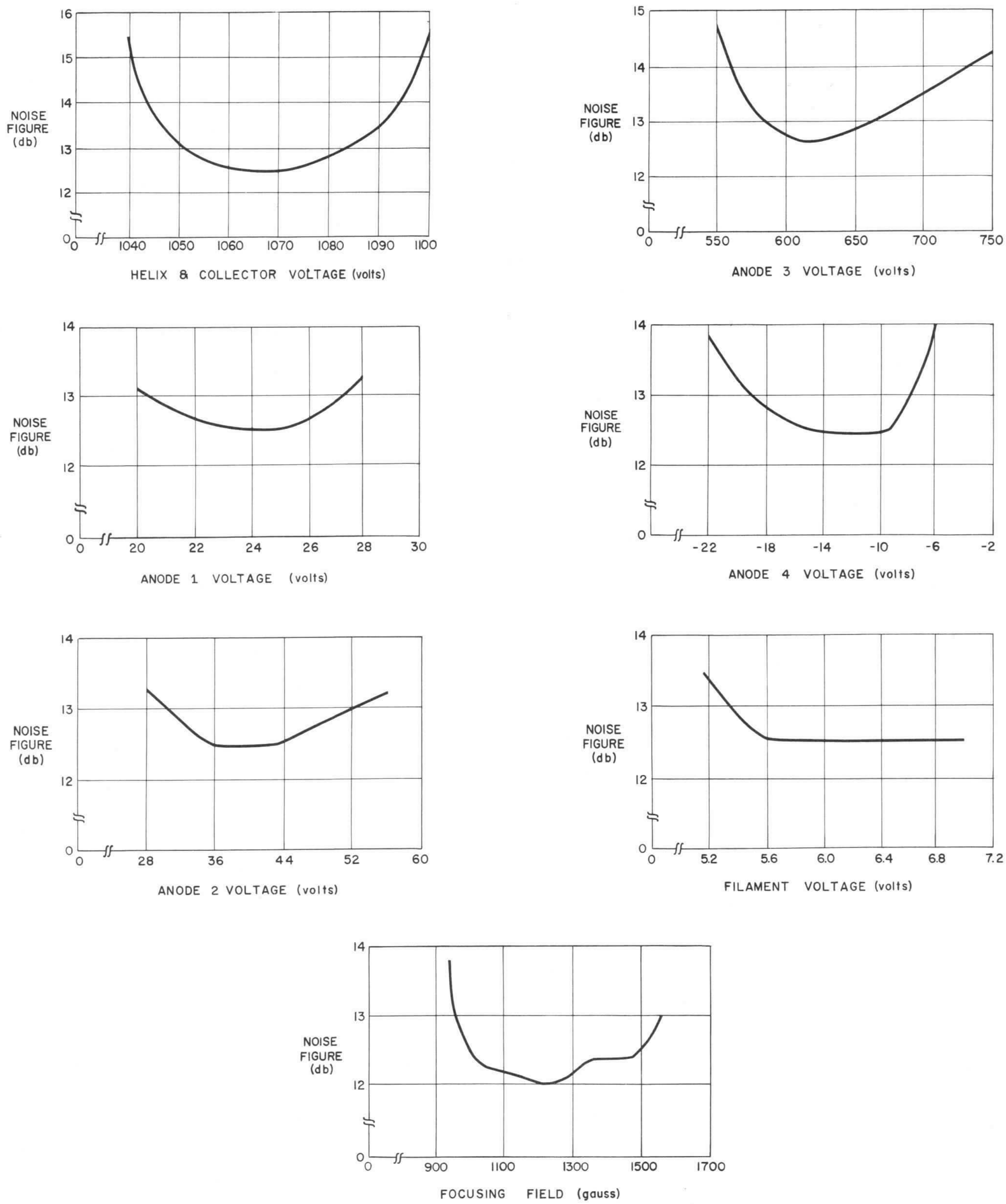

HA – 43 (DATA TAKEN AT 12.0 KMC)

FREQUENCY RANGE, 12.0 TO 18.0 KMC; NF, 17 DB MAX; S–S GAIN, 25 DB MIN; POWER OUT, 0 DBM MIN

OPTIMUM PARAMETERS

V_{A_1} = 25 V, V_{A_2} = 42 V, V_{A_3} = 620 V, V_{A_4} = −10 V, V_H = 1070 V, V_C = 1070 V, V_F = 6.3 V, AND B = 1000 GAUSS

FIGURE 4. HA – 43, NOISE FIGURE VS. OPERATING PARAMETERS

HUGGINS LABORATORIES
ENGINEERING NOTES

VOL. II, NO. 4 DECEMBER, 1963

Published by Huggins Laboratories Sunnyvale, California

INFRARED RADIOMETRY

R. J. Burke*

All bodies above absolute zero radiate energy continuously. The intensity of this radiation and its wavelength distribution are a function of the absolute temperature of the body and of its surface emissivity. These facts make possible the measurement of temperature by a radiometer which is focused on the object from any convenient distance. This Engineering Note presents some of the basic physical principles involved and discusses the practical methods of using radiometry for temperature measurement and control in industrial processes.

RADIATION

In 1792 Prevost proposed his famous theory of exchanges: all bodies interchange energy continuously as a result of radiation and absorption. If several bodies are housed in an enclosure and are all at a uniform temperature, each body absorbs from its surroundings an amount of energy equal to that which it radiates. Through this process each body is maintained at a constant temperature. All energy, of course, is conserved in the total reaction.

Energy interchange between solids or liquids takes place through the process of thermal radiation. Thermal radiation has a continuous spectrum; i.e., all frequencies are present in the radiation. Gases and vapors, on the other hand, normally radiate in what is called characteristic radiation, which has a discontinuous spectrum with characteristic intense lines that are uniquely related to the molecular structure of the radiating substance. In this Engineering Note we will deal only with thermal radiation and, hence, with the temperature measurement of solids and liquids.

BLACK BODY

In order to treat the problem of thermal radiation, the black body concept must be stated. Such a body does not exist in nature, but the concept implies that a black body absorbs all of the radiant energy incident upon its surface. This means that its absorptivity is unity and its reflectivity is zero. The sum of absorptivity and reflectivity is always unity. Some materials, such as black velvet and lamp black, reflect only a very small fraction of the incident radiation; thus, they approximate a true black body.

A black body can be more closely approximated by a very small opening in one wall of a hollow enclosure. Radiant energy entering the opening will be reflected many times within the enclosure and will, therefore, be eventually absorbed. As long as the dimensions of the opening are small compared to the internal dimensions of the enclosure, the opening will have the characteristics of a black body and will absorb all incident radiation.

*Manager, Systems Division, Huggins Laboratories, Inc.

A conical reentrant cavity, such as that illustrated in Figure 1, is often utilized to simulate a black body. As long as the cone angle is less than 30°, the cavity will be essentially black regardless of the material surrounding it.

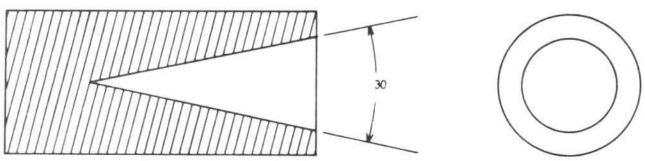

Figure 1. A Conical Reentrant Cavity Simulates a Black Body When Cone Angle Is Less than 30°.

EMISSIVITY

The quantity designated emissivity (ϵ) is unity for a black body and less than unity for all physically realizable surfaces. The quantity is dimensionless and is defined by the Stephan-Boltzmann law:

$$E = \epsilon \sigma T^4$$

where, E = total emissive power in watts per square centimeter per hemisphere
σ = Stephan-Boltzmann constant, 5.7 x 10^{-12} watts per square centimeter per degrees to the fourth power
T = absolute temperature, degrees Kelvin

The Stephen-Boltzmann law says that the total emissive power of a black body is proportional to the fourth power of its absolute temperature, the constant of proportionality being the Stephan-Boltzmann constant sigma (σ). When the body is other than a black body, total emission must be reduced proportionately and the emissivity reduces to:

$$\epsilon_x = \frac{E_x}{\sigma T^4}$$

This is the same as saying that the total emission per square centimeter from a real surface is less than that which would be emitted by a black body at the same temperature. The ratio of these emissions is the emissivity.

PLANCK'S LAW

Max Planck derived a radiation law which states that the emissive power of a unit area in the small wavelength interval delta-lambda ($\delta\lambda$) at any given wavelength λ is related to the wavelength and the absolute temperature by the following relationship:

$$J_\lambda = \frac{A}{\lambda^5} \frac{1}{e^{B/\lambda T} - 1}$$

where, J_λ = emissive power of unit area in the wavelength interval $\delta\lambda$
A = 3.732 x 10^{-12} watt cm^2
B = 1.436 cm degrees
λ = wavelength in cm
T = absolute temperature, °K

Figure 2 shows the relationship of emitted energy as a function of wavelength for a black body at various absolute temperatures. Several points should be noted about the distribution of energy as the temperature changes:

1. Total emissive power is the integral of J_λ over all wavelengths from 0 to infinity, and this integral is equal to σT^4. Consequently, the area under each curve increases rapidly with temperature.

2. The amount of energy radiated at any one wavelength increases monotonically with temperature. It is this relationship that provides a function which permits a radiometer to determine the temperature of a body by measuring its radiant flux in a given wavelength band.

As indicated by the shaded area in Figure 2, the wavelength band of the Model 3100

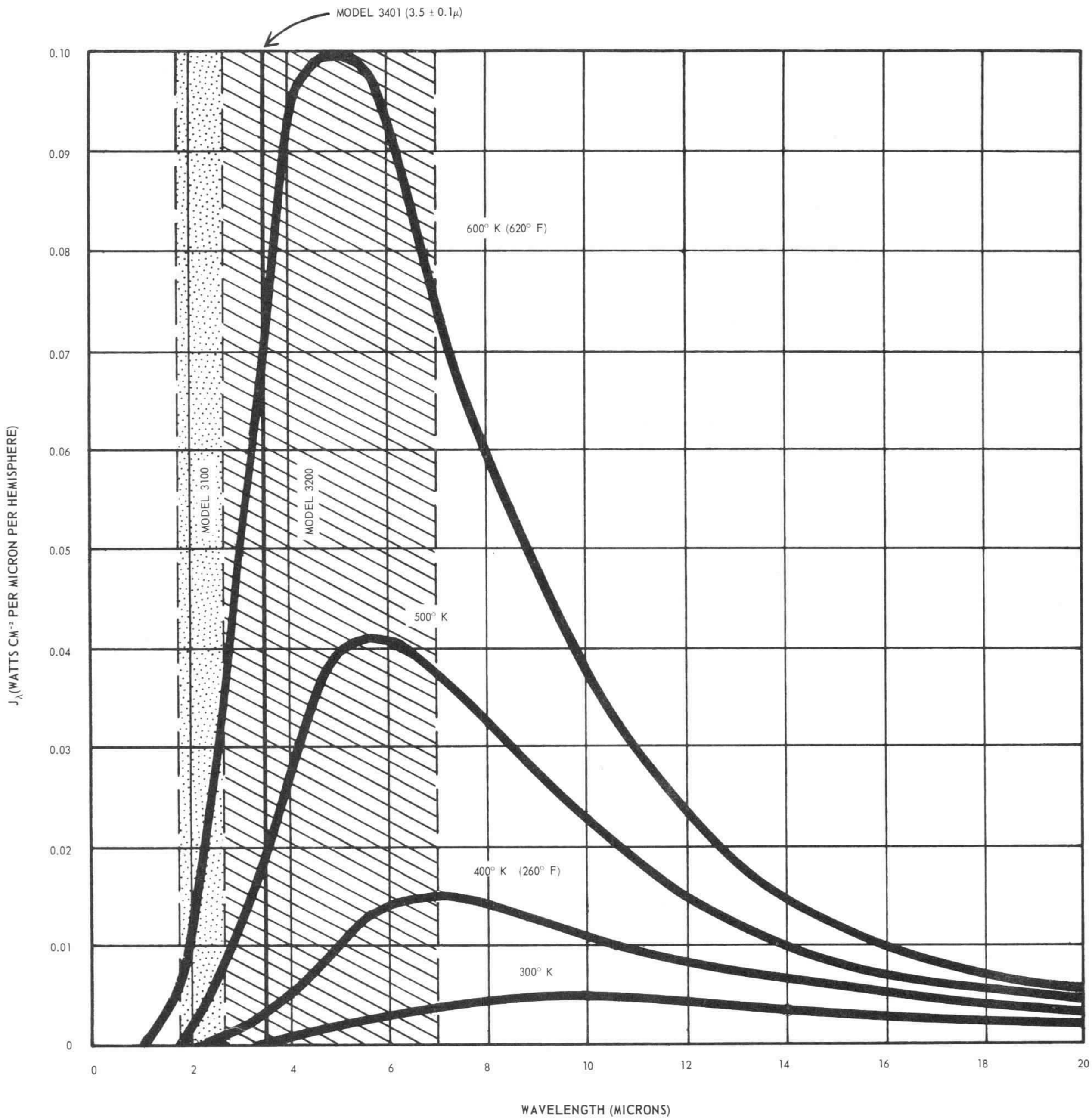

Figure 2. Spectral Distribution of Energy Radiated by a Black Body.

series Infrascope is 1.8 to 2.7 microns. It can be clearly seen why the lowest usable temperature on the Infrascope is 140° F (333° K). The wavelength band of the Model 3200 radiometer is also shown by the cross-hatched area, and as can be seen, the lowest usable temperature is -80° F (211° K).

3. As the temperature increases, the left hand side of the distribution curve moves to shorter wavelengths. This explains why a body at 1300° F is called "red hot," for it radiates sufficient energy in

the 0.7 micron band (wavelength which the eye identifies as red) for the eye to detect.

When the temperature rises to 2700° F, wavelengths as short as 0.4 microns are present in the radiation. The combination of all radiation between 0.4 and 0.7 microns includes all colors from red to violet and appears to the eye as white. Thus, at this temperature we refer to the body as being "white hot."

4. As the temperature of the body increases the shape of the spectral distribution curve changes such that the maximum radiation shifts to shorter and shorter wavelengths.

RADIOMETERS

The radiometer utilizes radiation from any hot object to determine the object's temperature. As can be seen in Figure 2, the amount of energy being radiated from each square centimeter of the surface of a body within the wavelength band of the radiometer is an exact and known function of the temperature, providing the surface is black. If the surface is not black a correction must be made for emissivity, a quantity that must be known from previous experiment or measured for each case.

Table 1. Emissivities of Some Representative Surfaces.

MATERIAL	TEMPERATURE in degrees Fahreinheit	EMISSIVITY
Earth	Ambient	0.98
Foliage	Ambient	0.98
Water	Ambient	0.98
Ice	Ambient	0.98
Brick	Ambient	0.98
Stone	Ambient	0.98
Granular Paint Pigment (any color)	Ambient	0.92
Cloth	Ambient	0.98
Wood	Ambient	0.98
Skin	Ambient	0.98
Aluminum (highly polished)	Ambient	0.08
Aluminum (oxidized)	400	0.11
Aluminum (roughened)	300	0.70
Brass (burnished)	200	0.05
Brass (oxidized)	200	0.07
Steel (clean, gray)	300	0.60
Steel (scrubbed with steel wool)	300	0.46
Steel (pickled in HCl)	300	0.35
Steel (buffed bright)	300	0.11
Carbon (rough plate)	200	0.77
Carbon (rough plate)	900	0.72

Table I lists the emissivities of some representative surfaces under typical conditions and shows the primary dependence upon surface roughness. In utilizing a radiometer the following rules are most important to be observed in order to obtain accurate readings:

1. The object under observation must fill the field of view of the instrument. Radiometers, such as that shown in Figure 3, manufactured by Applied Systems Corporation (a subsidiary of Huggins Laboratories) are all equipped with reticles in the field of view which define the area under observation. Accurate measurement requires that the reticle image must be completely inscribed within the outlines of the object under measurement. If any part of the field of view, as defined by the reticle, is not subtended by the target object, the temperature reading will be a weighted average between the temperature of the object and that of the background visible in the reticle.

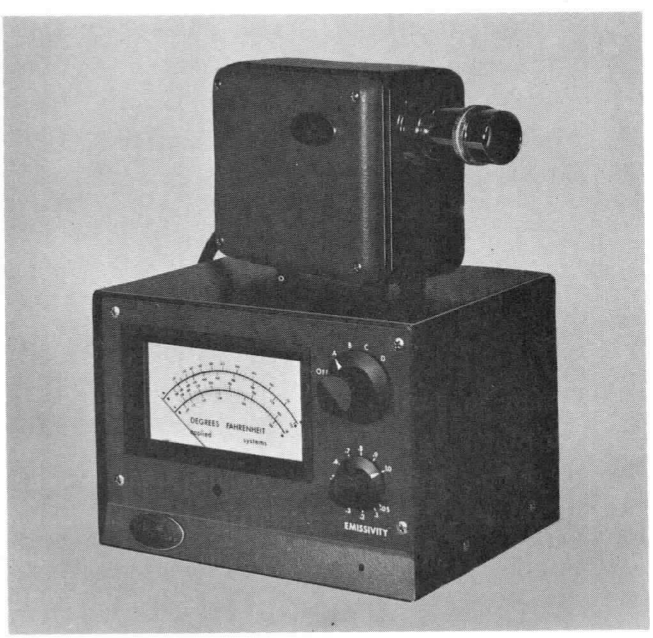

Figure 3. Model 3121 Infrascope.

2. A target object must be opaque in the wavelength band of the radiometer. If the material is transparent in this wavelength band, the temperature reading will be primarily that of the background visible behind the target object.

   In the measurement of plastic films, for example, the Model 3401 radiometer must be used. The 3401 has a narrow wavelength response around the 3.5 micron band at which all plastics containing carbon and hydrogen are opaque. The Model 3100, on the other hand, sees right through the plastic, for this material is transparent in the 1.8 to 2.7 micron band.

3. Any surface which is not black has some reflectivity, so care must be taken to avoid the reflection of radiant energy from nearby lights, radiant elements, or the sun. The radiometer can react only to the total radiant energy coming from the surface and cannot differentiate between thermal radiation due to the temperature of the body and energy reflected from some other source. In most cases the small area to be observed by the radiometer can be shadowed from other sources by appropriate placement of the radiometer or screening materials. A tube with one end close to the target object with the radiometer sighted through the bore is often a good solution to reflective interference. Such a tube should preferably be made of a material which is not shiny on the inside.

4. The emissivity of the surface must be considered. Emissivity is usually and most readily obtained from either the tables supplied or by means of a single, simple measurement. If the body can be measured at some known temperature, the emissivity is found immediately by setting the emissivity dial to that point

which brings the radiometer into agreement with the known temperature. It will then track within the prescribed accuracy of the instrument for all other temperatures.

Another method for measuring emissivity, or dispensing with it, is illustrated in Figure 4. If a highly reflective surface can be mounted around the target object at any convenient distance and in such a way that the radiation from the object will be repeatedly reflected, a cavity is formed which effectively becomes a black body. Measurement of the body temperature can then be made directly with the emissivity set at 1, or a comparison of the temperature reading without the reflector to the equivalent reading with the reflector will provide the emissivity.

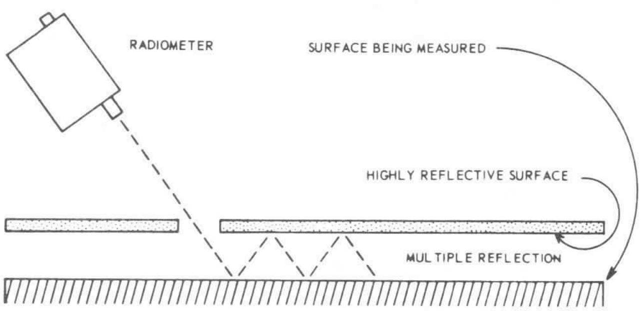

Figure 4. Use of a Highly Reflective Surface Around the Target Object Eliminates Emissivity Factor.

5. The angle at which the surface is viewed is not important to accuracy, for each increment of area radiates into its surrounding volume in a pattern which falls off from the normal (perpendicular) by the cosine of the angle from the normal. Since the amount of area subtended by the reticle increases directly as the cosine of the viewing angle, the two effects cancel each other. The net result is that the amount of energy entering the aperature of the radiometer from the body is independent of the angle to the surface so long as the object continues to fill the aperature. Radiation into the aperature drops off with cosine θ, and the area subtended in the field of view increases with cosine θ. As shown in Figure 5, the effects cancel.

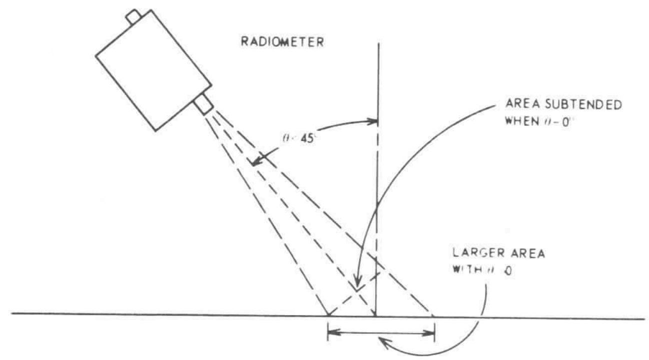

Figure 5. Effects of Radiation into the Aperature of the Radiometer and the Area Subtended in the Field of View as a Function of θ Cancel. Thus, Measurement Is Independent of θ.

6. In many industrial process control applications the reproducibility of a given temperature is of greater importance than the absolute value of the temperature. In such cases, determination of the emissivity is of little value, and the emissivity setting may be left at unity.

7. Because radiant energy, which is measured by the radiometer, is a fourth power function of the temperature and only a first power function of emissivity, an error of 5% in the emissivity setting produces only a 1% error in the temperature indication. For this reason emissivity should not be considered a difficult problem in using the radiometer for temperature measurement. In particular, the question has been raised concerning the repeatability of the emissivity setting on the radiometer to an accuracy of 1 or 2%. From the fore-

going discussion it becomes clear that the coarseness of the emissivity setting does not significantly degrade the instrument's accuracy.

8. It often becomes necessary to make temperature measurements through a window. The effect of absorption by the window is identical to that due to a change in surface emissivity and can consequently be compensated for by the emissivity setting. Measurement of any object of known temperature through the window provides the information required for properly setting the emissivity compensator.

SUMMARY

A radiometer measures the incident radiant flux within a fixed wavelength band. When its field of view is filled with a single object, the reading of the radiometer is a function only of the temperature and the emissivity of the surface of the object. Emissivity of a surface can be determined by one of several comparatively simple measurements or from predetermined tabulated values. With the appropriate emissivity setting, the radiometer will indicate temperature accurately over the entire range for which it is designed. Care must be taken, however, to ensure against reflections from the surface under measurement or from some reflective point within the instrument's field of view.

HUGGINS LABORATORIES
ENGINEERING NOTES

VOL. II, NO. 5 MARCH, 1964

Published by Huggins Laboratories Sunnyvale, California

THE TEN MOST-ASKED QUESTIONS ON INFRARED

Burton Bernard *

1. What Is Infrared Radiation?

Infrared radiation is electromagnetic radiation of frequency above that of radio frequencies and below that of visible frequencies (Figure 1). Like all electromagnetic radiation, it travels at the speed of light (186,000 miles per second), and can be measured either in frequency or wavelength (usually microns, or 10^{-6} meter).

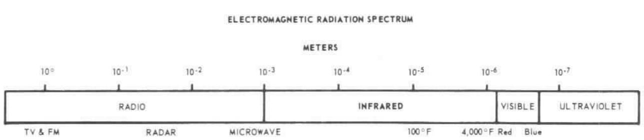

Figure 1. Frequency Spectrum.

2. Does a Substance Have To Be "Hot" To Emit Infrared Radiation?

No. All objects emit infrared radiation which is related to the temperature of the object. Only at absolute zero (–273° C) will an object cease to emit any radiation, including infrared radiation. The following formula shows the relationship between the total energy emitted by an object and its temperature:

$$W = \epsilon\sigma T^4 \qquad (1)$$

where W = radiant flux density; ϵ = emissivity factor (discussed in Question 5); σ = Stefan-Boltzmann constant (5.67×10^{-12} watts/cm^2-deg^4); and T = absolute temperature in degrees Kelvin.

3. Does The Amount Of Infrared Radiation Vary With Temperature?

Yes. Infrared radiation is emitted over a wide band of wavelengths, but the amount of energy emitted at any one wavelength increases as the temperature is increased (Figure 2). The wavelength of the energy peak decreases as the temperature is increased. Mathematically:

$$\lambda = \frac{2.96 \times 10^3 \text{ microns}}{T} \qquad (2)$$

where λ = peak wavelength in microns, and T = temperature in degrees Kelvin.

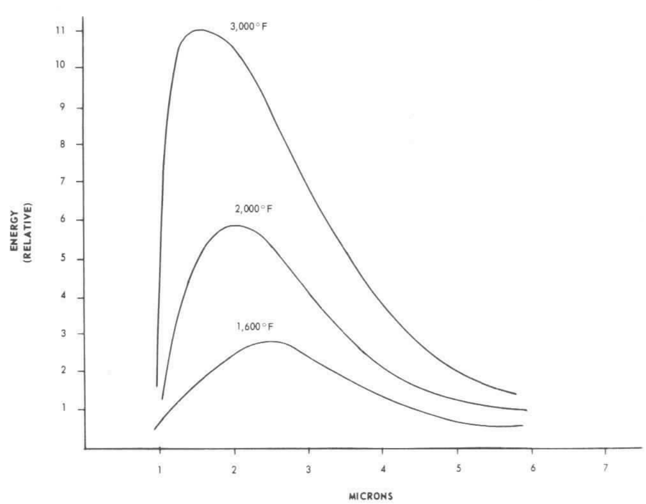

Figure 2. Spectral Distribution of Radiated Energy.

*Sales Manager, Infrared Products, Huggins Laboratories

Reprinted from May, 1961 issue of *Instruments & Control Systems*

4. What Is A Blackbody?

A blackbody is a surface or object which completely absorbs all of the radiant energy striking it. According to Kirchoff's Law, the radiant absorption (A) of an object must equal the radiant emittance of that object, or:

$$A = \epsilon \tag{3}$$

As there are no perfect blackbodies found in nature, an emissivity factor ϵ must be determined to solve for W in Equation 1.

5. What Is Emissivity?

Emissivity is the ratio of the radiant energy emitted by an object at a temperature T to the radiant energy emitted by a blackbody at the same temperature T. This can be written as:

$$\epsilon = W_o/W_{bb} \tag{4}$$

where ϵ = emissivity factor, W_o = energy emitted by an object at a temperature. W_{bb} = energy emitted by a blackbody at the same temperature.

6. What Is the Relationship Between Emissivity, Reflectivity, Transmissivity, and Absorptivity?

If an object does not absorb all of the radiant energy falling upon it, it must reflect and/or transmit the remaining energy. The sum of absorptivity, (A), reflectivity (R), and transmissivity (T) must equal 100% of the total incident energy, or

$$A + R + T = 1 \tag{5}$$

$$A = \epsilon = R-(R + T) \tag{6}$$

7. Does Emissivity Vary With Wavelength?

The emissivity of some objects does change with wavelength. The amount and direction of change of the emissivity factor varies with different types of materials. Figure 3 shows a few common materials and their respective emissivity factors at various wavelengths.

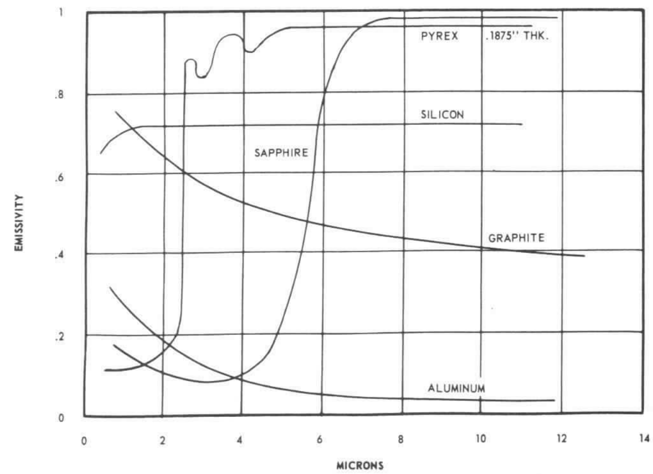

Figure 3. Emissivity Factor Varies with Different Types of Material.

8. How Can Infrared Energy Be Detected?

There are two general classifications for infrared detectors—one is the *thermal detector* and the other is the *photodetector.*

Operation of the *thermal detector* is based on the change of a physical property (such as resistance or thermoelectric force) of the detector as its own temperature is changed. Examples of thermal detectors are thermocouples, pneumatic detectors, and bolometers.

The infrared *photodetector* is a semiconductor which produces a signal proportional to the photon flux which strikes its sensitive element. Photodetectors include photoconductive, photovoltaic, and photoelectromagnetic detectors. The detectivity of a photodetector can be increased by cooling.

Both thermal and photo detectors are used frequently with an optical system employed to focus the radiant energy onto the sensitive element. The thermal detector, which has a uniform spectral response to infrared radiation, does not respond as rapidly to thermal changes as does the photodetector. Figure 4 shows the relative response curves of some of the more familiar types of detectors being used today.

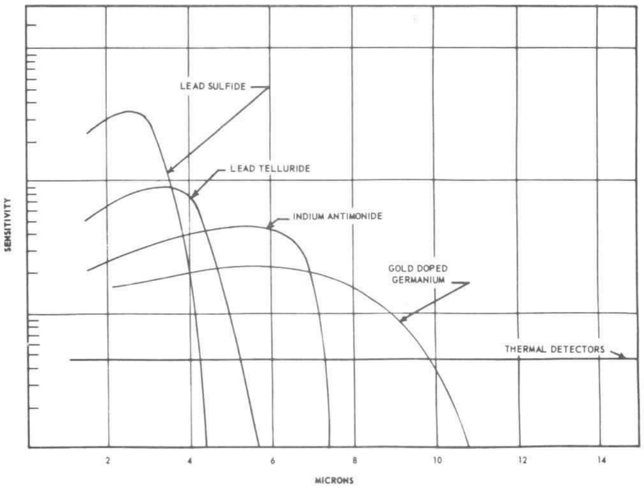

Figure 4. Relative Response Curves of Various Infrared Detectors.

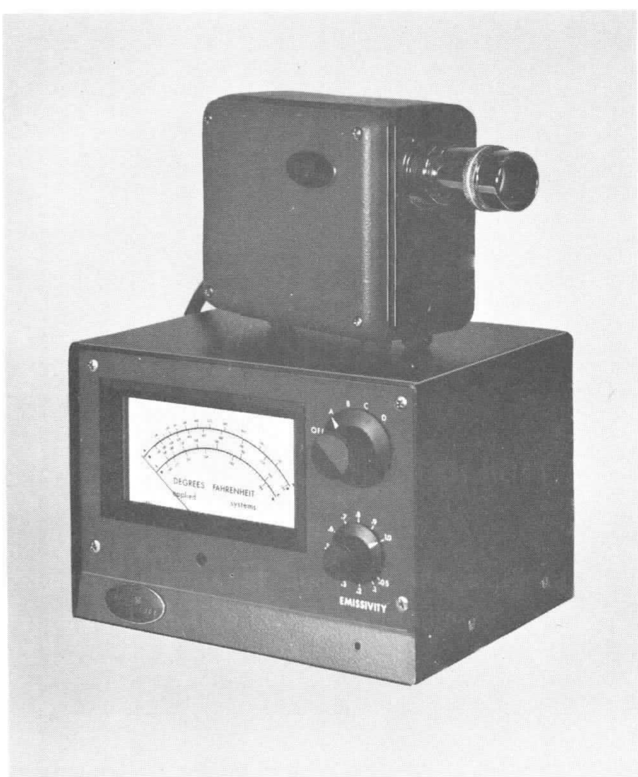

Figure 5. Huggins Mark IX Infrascope Radiation Thermometer.

9. Is There Any Limit On The Range At Which An Object's Temperature Can be Measured By An Infrared System?

For normal industrial applications the maximum range depends only on the size of the object and the resolution angle of the infrared optical system. For example the Infrascope (Figure 5) has a resolution angle of less than ½ degree and can resolve a spot size approximately 1" by 1" at a distance of 10 feet, or 2" by 2" at 20 feet, etc. If the object is not completely resolved, its radiant energy will be integrated with the surrounding energy and result in a temperature reading different than that of the object. If, however, the temperature and resolved area of the surroundings are known, then an accurate temperature reading can be determined at any distance.

10. Does The Amount Of Emitted Infrared Energy Vary With Angle?

Yes. As stated in Lambert's Law, the radiant energy emitted by some objects and surfaces in any one direction varies as the cosine of the angle between the normal and that particular direction. That is:

$$W_\theta = W_n \cos\theta \qquad (7)$$

where W_θ = total energy emitted in any one direction; W_n = total energy emitted in a normal plane; θ = angle between the normal and direction of emittance.

However, as the radiation thermometer does not "see" a point source, but resolves a definite spot size, the area resolved increases by cos θ as the angle from the normal increases, or

$$A_\theta = A_n/\cos\theta \qquad (8)$$

where A_θ = area resolved at a given angle to the normal; A_n = area resolved at the normal.

From equations 7 and 8 it can be shown that for any given temperature, regardless of the angle of incidence, the amount of flux density detected by the radiometer will remain the same because

$$P_n = W_n A_n \tag{9}$$

where P_n = radiant power emitted in a normal plane (watts); W_n = radiant emittance at a normal plane (watts/cm^2); A_n = area resolved in a normal plane (cm^2).

By substitution:

$$P_n = W_\theta A_\theta \cos\theta/\cos\theta \tag{10}$$

$$P_n = W_\theta A_\theta = P_\theta \tag{11}$$